Hindawi

Research Article

Seismic Analysis and Damage Evaluation of RC Frame Structures Based on BIM Platform

Feng Wang [1] **and Qiang Chen** [2]

^{1}*College of Civil Engineering, Dalian Minzu University, Dalian 116600, China*
^{2}*Digital Design BG, Glodon Pegatron Corp., Beijing 100193, China*

Correspondence should be addressed to Feng Wang; wfeng@dlnu.edu.cn

In order to overcome the shortcomings in integrating the building information modeling (BIM) and seismic finite element technique for building structures, a new seismic analysis and damage evaluation method for reinforced concrete (RC) frame structures was proposed by integrating Revit and OpenSees, in which the information about geometric and material of the existing BIM model in Revit was extracted as part of the finite element analysis model of OpenSees; supplementary settings about the element type, material constitutive model, load information, and analysis type for finite element analysis were made according to the input format of OpenSees, and OpenSees program was directly called for numerical analysis in the Revit software which realized seismic analysis and damage evaluation of RC frame structures based on BIM. RTO, a revolutionary structural seismic analysis and damage evaluation tool based on the three-tier architecture theory, was created by combining Revit and OpenSees via the RevitAPI interface. The preprocessing module was created to contact OpenSees for finite element analysis, the postprocessing module was created to secondary analyze, display, and export the analysis data, and crucial structural seismic damage information was automatically saved in the Revit model. A calculation example of a five-story RC frame structure was provided to demonstrate the operation process of the proposed method and the developed program. The example proved the feasibility of integrating the BIM and finite element method in elastic-plastic structural seismic analysis. The proposed approach would facilitate the participation of structural seismic analysis in BIM life cycle collaboration.

1. Introduction

With the rapid development of information technology in recent years, the building information model (BIM) has been extensively used to achieve information sharing and collaboration management in different construction engineering fields. BIM presents an important direction for future informatization development in the construction industry; however, functions of different mainstream BIM software are very limited. Data conversion between different professional construction software packages generally needs to be carried out through the IFC standard to realize BIM-based data sharing and collaboration [1–5]. At present, the research on integration or data conversion between BIM and various engineering software has developed rapidly. The corresponding fields involved in these types of software include construction management [6], cost management [7], structural design and analysis [8], energy efficiency analysis [9], and VR simulation [10].

In order to realize structural design and analysis on the BIM platform, model data conversion between BIM software and structural analysis software has been explored. Zeng et al. [11] transformed a BIM model into a model that could be read by different structural software through programming to solve the missing data problem in data conversion using the IFC standard. Barazzetti et al. [12] proposed a method of converting the BIM model of ancient buildings into a structural finite element model. Some scholars have presented the structural design method based on the BIM model. Dong et al. [13] discussed the design process of structures based on the BIM platform and analyzed the advantages of the BIM design method by comparing with the

traditional structural design method. Tafraout et al. [14] applied structural optimization design to the BIM platform and proposed a method to realize the automatic design of RC wall-slab structures on the BIM platform with a genetic algorithm. Some scholars combined mainstream BIM software with a fire dynamics simulator (FDS) to analyze structural fire responses. Xu et al. [15] converted a BIM model into an FDS model to realize rapid creation of a fire hazard numerical analysis model and conduct a post-earthquake fire hazard simulation based on FEMAP-58. Based on the IFC standard, Shi et al. [16] realized the rapid and accurate information sharing of building fire safety analysis between BIM software and mainstream fire simulation software.

So far, although some progress has been made in model data conversion between BIM and structural analysis software, functions are still limited to the transformation of geometric and material information. Thus, information related to load, constraint, analysis element, material constitutive and analysis parameter, and so on still needs to be set up in structural software.

The Eurasian seismic band and the Pacific rim seismic belt encircle China, and earthquakes are common. The hazard of earthquakes to economic development has grown significantly. Therefore, it is important to continuously develop and improve seismic theories and methods for buildings. In recent years, BIM has been combined with seismic analysis technologies to explore BIM-based analysis methods for earthquake-induced structural damage evaluation. Lee [17] explored how to obtain the information of the Revit model through an IFC format file and convert it into an OpenSees readable file, which provided a reference for the integration of OpenSees into the BIM platform. Mehdi et al. [18] explored how to establish the OpenSees model through the BIM model and proposed a seismic damage assessment method of structures based on BIM. Anil et al. [19] and Zou et al. [20] proposed new methods based on BIM for seismic structural damage assessment. Perrone and Filiatrault [21] discussed the effectiveness of adopting a BIM model for seismic design of nonstructural components and developed a simplified tool to directly conduct seismic design of nonstructural components.

In the research on the integration of BIM and structural earthquake resistance, the postearthquake repair and the seismic reconstruction have become the important research direction concerned by scholars. Vitiello et al. [22] proposed a simplified method for cost optimization of seismic reinforcement strategy of existing buildings based on BIM, which aimed to optimize the seismic reconstruction strategy in the BIM platform while taking into account safety and economy. Xu et al. [23, 24] combined BIM software with finite element analysis software to explore a BIM-based building earthquake loss prediction method based on FEMAP-58. Xu et al. [25] proposed a 5D simulation method of postearthquake repair of buildings based on BIM in order to provide guidance for the postearthquake repair process, in which the repairs were associated with the building model to be repaired, repair time, and repair cost. Caterino et al. [26] discussed the advantages of BIM in multicriteria decision-making and proposed a decision-making method of seismic optimization and reconstruction of buildings based on BIM.

Furthermore, the studies of BIM in conjunction with other new technologies have progressed quickly. Reem et al. [27] developed a novel method for leveraging laser scanning technology to generate a BIM model of earthquake loss based on existing BIM models. Musella et al. [28] applied BIM and artificial intelligence technology to the seismic damage evaluation of existing buildings, in which the graphic recognition and classification technology was applied to obtain the building visual damage data. The method provided a new way for evaluating, designing, and managing the seismic repair process of existing buildings.

At present, the research and application of BIM-based seismic analysis and evaluation for building structures are still in the early stage, and most research works cannot realize the integration of BIM and seismic analysis functions. The integration of structural design, analysis, and evaluation into BIM to realize BIM data sharing and analysis is a topic that requires further research in construction engineering.

In order to realize the seismic analysis and evaluation of reinforced concrete (RC) frame structures based on BIM, this work proposed a novel method by integrating the Revit program and the OpenSees program. In order to call OpenSees on the Revit platform, a program called RTO was developed through the Revit API interface using the C# language, through which the analysis data of OpenSees were postprocessed, and critical structural damage data were stored in the Revit model. The proposed approach could provide a solution for structural seismic analysis to participate in BIM full life cycle collaboration.

The following is the paper's organization paragraph: the overall research framework is proposed in Section 2. The function and principle of the developed program are introduced in Section 3. The developed program is examined, and the analysis results are discussed by a calculation example in Section 4. Finally, the conclusions are given in Section 5.

2. Overall Research Framework

The RTO software was built using a three-tier design [29] and was customised to fit different application scenarios. The program's core design mentality was made up of four elements: preprocessing, postprocessing, damage information storage, and visual display (Figure 1).

The design architecture of preprocessing component is shown in Figure 2, and the design architecture of the components of postprocessing, damage information storage, and visual display is shown in Figure 3.

2.1. Preprocessing. The component of preprocessing includes three steps:

(1) The geometrical, cross-sectional, and material information of structures and components was directly extracted from the Revit model to fulfill the modeling requirements of OpenSees
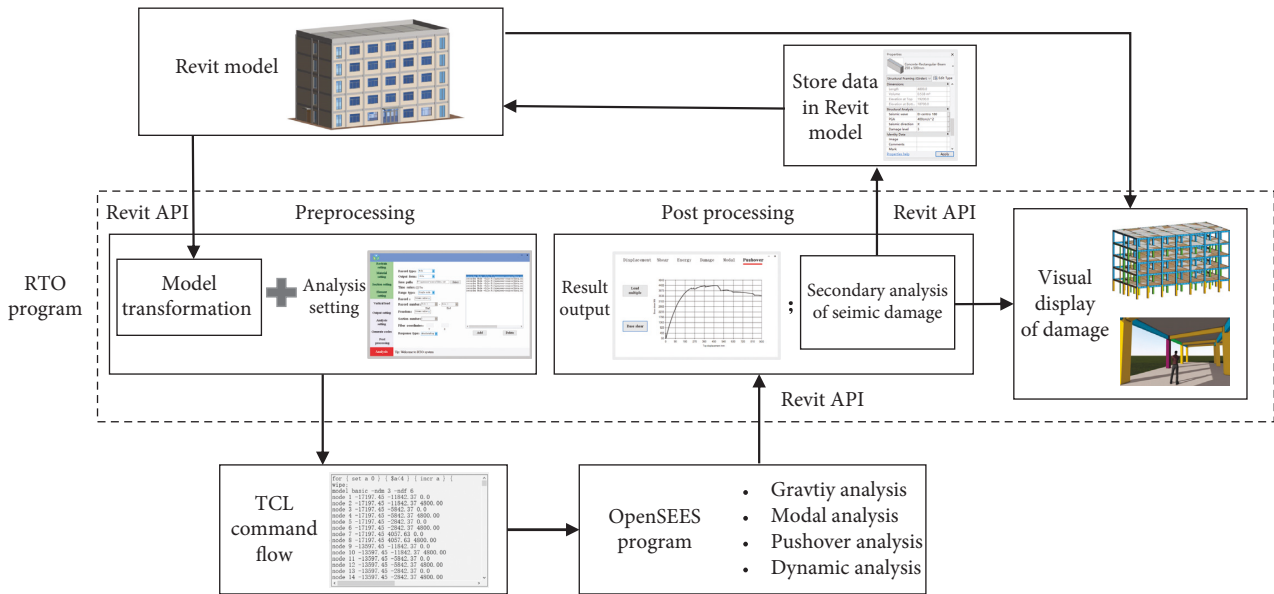
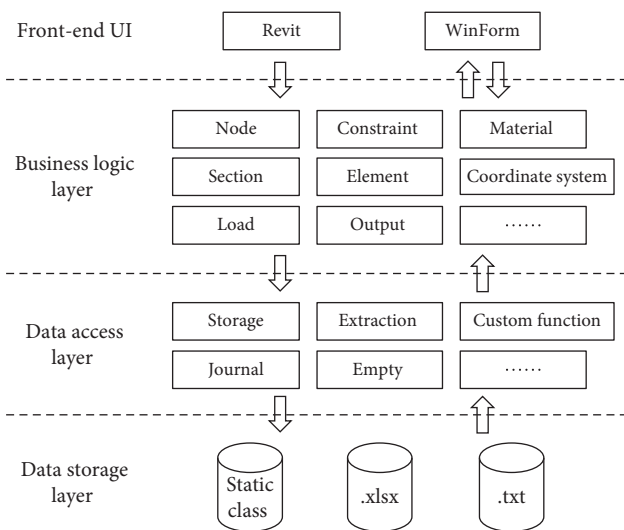Figure 1: Design mentality of the RTO program.

Figure 2: Design architecture of preprocessing component.

(2) According to the analysis setup requirements of the OpenSees program, vertical load setup, analysis model selection, component cross-sectional information setup, and analysis parameter setup were carried out in Revit software

(3) The TCL command flow was directly generated from extracted Revit model data and front-end analysis setup data. OpenSees was called to read the TCL command flow for structural finite element analysis.

2.2. Postprocessing. The component of postprocessing includes two steps:

(1) Structural analysis data obtained from the OpenSees program were read and displayed in the form of figures, tables, or documents
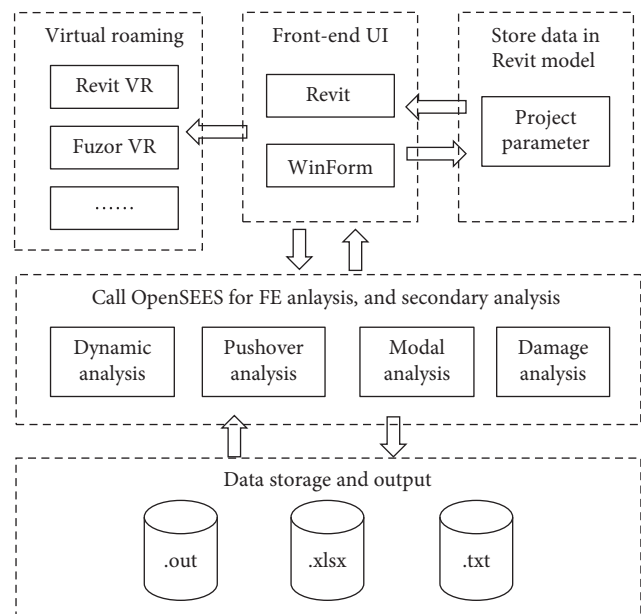

Figure 3: Design architecture of the components of postprocessing, information storage, and visual display.

(2) According to structural seismic performance analysis and evaluation requirements, OpenSees output data were read for a secondary analysis, seismic damage evaluation of RC frame structures

2.3. Damage Information Storage and Visual Display

(1) Key structural seismic damage information was stored in the Revit structural model to facilitate the participation of structural seismic analysis in BIM life cycle collaboration

(2) According to the damage level of components obtained by postprocessing analysis, each component

model was automatically color marked, and then, the Revit structural model was visually displayed through the methods of 3D view and virtual roaming.

3. Research and Development of Program

3.1. BIM Model Data Extraction. The geometric model data conversion from Revit to OpenSees was realized through the preprocessing component. Structural analysis parameters were set up accordingly, and the conversion from the BIM model of Revit to the finite element model of OpenSees was considered as an extraction process of BIM model data. The logical process is shown in Figure 4.

3.2. Application of Vertical Load. The vertical constant loads of beams, columns, walls, and other components of a building were calculated automatically by matching the bulk density of the material and reading the geometric data and material type information of the Revit model. The vertical constant loads and varying loads of the roof slab and the floor were automatically transferred to supporting beams or walls in the form of a line load according to the load transfer rules of two-way slab or one-way slab, respectively. The representative values of the gravity load on each floor were automatically calculated and assigned to each node according to their loaded area. The computational algorithm for the automatic application of the vertical load is shown in Figure 5.

3.3. Human-Computer Interaction for Parameter Setting. The functions of seismic analysis setups and output data setups were designed in order to call the OpenSees program for finite element analysis, and the setup interface of the program is shown in Figure 6.

3.3.1. Material Property Setting. The Revit model only contained simple material type information without corresponding material mechanical properties in OpenSees; thus, direct material information conversion from Revit to OpenSees could not be carried out. Therefore, an interactive setup function for material mechanical properties was developed. Material type information in the Revit model was automatically read by the RTO program, and constitutive information of the corresponding material type at the material setup interface was selected, inputted, or modified and converted into a TCL command flow matching with the Revit model. In addition, the TCL command flow of the material property setup could be previewed at the interface for easy browsing and timely error correction.

3.3.2. Element Selection. An element selection function was developed to assign relevant analysis elements to the linkage model connecting each node based on the types of analysis elements provided by the OpenSees application. Plastic hinges of RC beam and column components were simulated using the elastic-plastic fiber model. This program could

automatically read geometric and material information at the cross-sections of structural components in the Revit model. Moreover, for longitudinal rebars at the cross-sections of structural components, this program automatically generated a rebar fiber command flow according to rebar coordinates and material properties. For the concrete in the cross-sections of structural components, concrete fibers were automatically generated by setting up cross-sectional meshes. The concrete in the core area was constrained by stirrups, and the concrete in the protective layer adopted different material constitutive parameters.

The modeling procedure of the elastic-plastic fiber model of component cross-sections through the redevelopment of Revit is as follows:

(1) The longitudinal rebar model of Revit was filtered by using "Filtered element collector," "Element category filter," and function "Where passes"

(2) All longitudinal rebars belonging to the same structural component were screened out

(3) The coordinates of each longitudinal rebar relative to the considered component cross-section were recorded

(4) The diameters of longitudinal rebars were obtained, and the cross-sectional areas of these rebars were calculated.

(5) The function "Createconcretefiber" was compiled to create concrete fiber, in which the sizes of cross-section and the number of fibers in the two orthogonal directions of the component cross-section were taken as the parameters of this function, and the coordinates of concrete fibers were determined.

3.3.3. Analysis and Output Setting. The RTO program directly called OpenSees in the Revit model to read the generated TCL command flow for gravity analysis, modal analysis, pushover analysis, dynamic time history analysis, and so on. The interactive function of parameter setups required by different analyses was developed in the front interface of the program.

3.4. Postprocessing Analysis and Visualization Display. In this subsection, the functions of the developed program about the postprocessing analysis output and visual display of earthquake damage were introduced.

3.4.1. Postprocessing Analysis Output. As the OpenSees program does not have postprocessing functions, OpenSees data are generally exported to other types of software for secondary analysis. However, the RTO program developed in this work included a postprocessing module for OpenSees data analysis. According to the analysis type and parameter settings selected in human-computer interactions, modal analysis, dynamic time history analysis, and pushover analysis were performed. Figures 7 and 8 show the displacement time history curve of structural roof and the
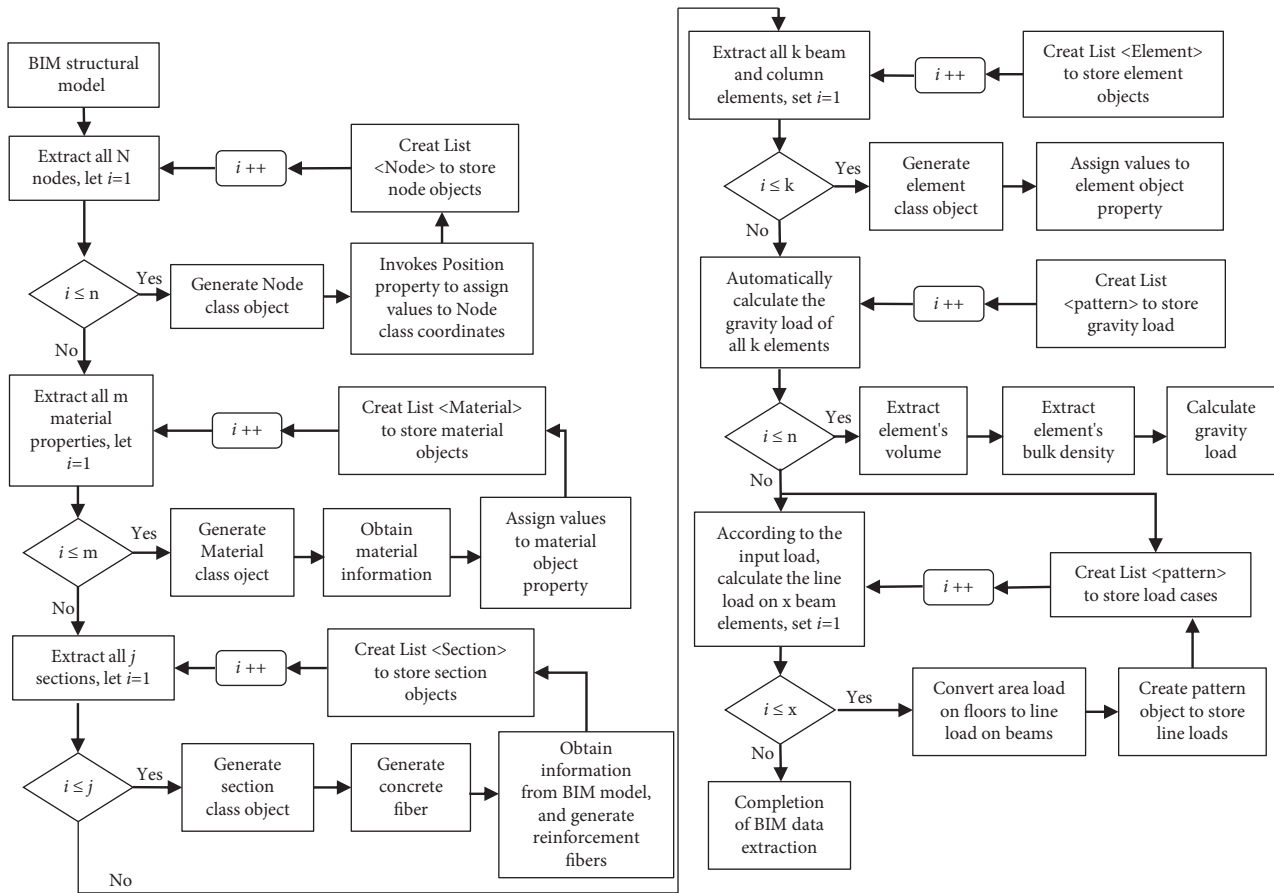
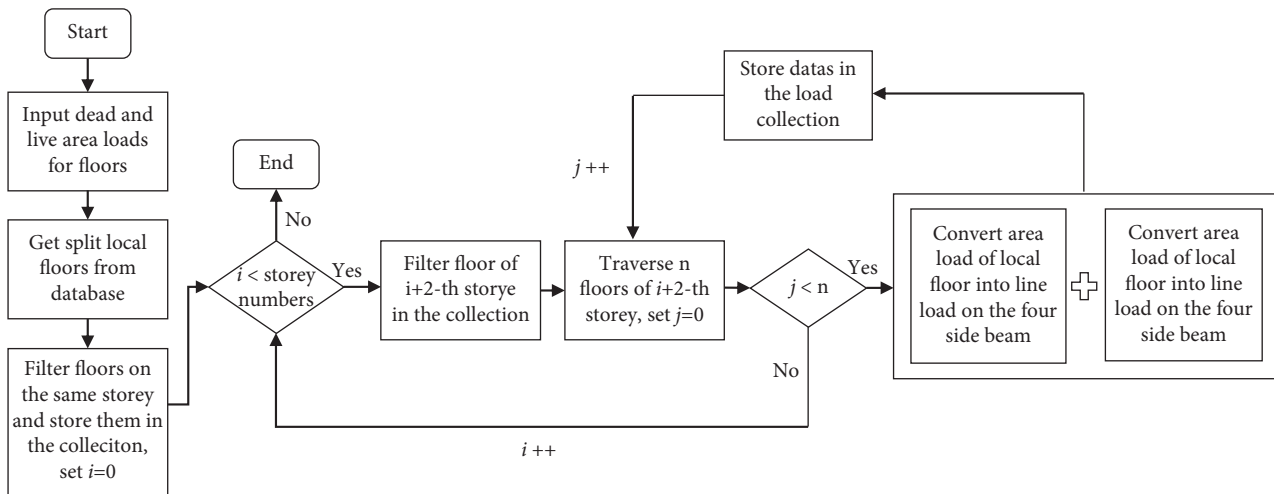FIGURE 4: Flowchart of Revit model data extraction.

FIGURE 5: Flowchart of the automatic application algorithm of vertical load.

pushover analysis capability curve obtained by the program, respectively.

3.4.2. Visual Display of Earthquake Damage.

According to the Standard for Seismic Resilience Assessment of Buildings [30], seismic damage levels for RC structural components could be determined by material strains in the cross-section of structural components. The material strain evaluation standards for different damage grades are given in Table 1. In this work, the strain values of longitudinal rebars and concrete in each plastic hinge area of a structure under an earthquake were obtained by calling OpenSees of the RTO program. The earthquake damage level of each structural
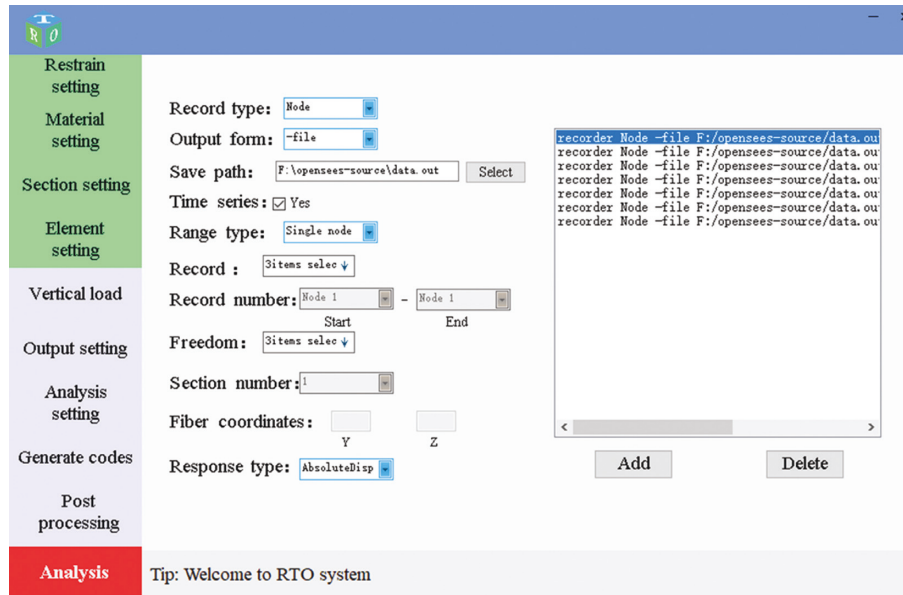
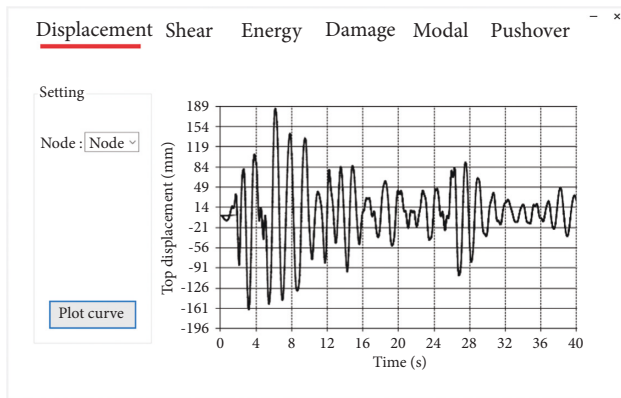FIGURE 6: Interface of program setup.

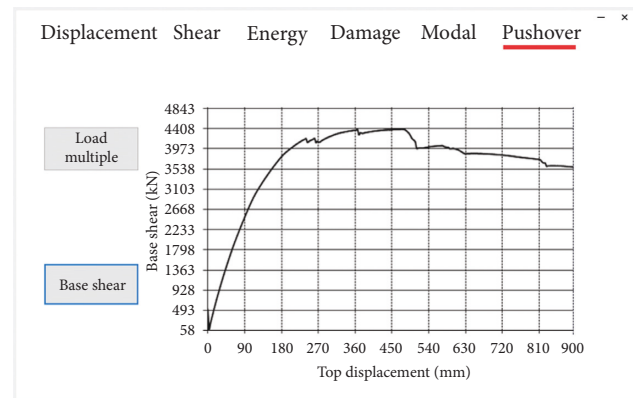FIGURE 7: Display diagram of displacement time history.

FIGURE 8: Display diagram of pushover capability curve.

component was identified by substituting related data into Table 1. The Revit redevelopment technology was used to automatically change the color of structural components according to different earthquake damage levels. The damage conditions and distribution characteristics of the structure under an earthquake were displayed in a 3D view of the Revit model. The relationship between seismic damage level and Revit model color is given in Table 1.

Furthermore, this Revit model with color annotations was put into virtual roaming software. A program user could perform a virtual travelling inside the building structure model to see the damage degree and distribution of each component in greater detail and check the seismic performance evaluation information for that component.

In Table 1, ε_1 is the principal tensile strain of rebars, ε_2 is the principal tensile strain of concrete, ε_p and ε_{cu} are the peak and limit strains of concrete under uniaxial compression, respectively, and ε_y is the yield strain of rebars. Moreover, level 0 implies no damage, and level 4 indicates the most serious damage.

3.5. Automatic Storage of Earthquake Damage Information in the BIM Model. Seismic performance data obtained from finite element analysis were automatically stored in the Revit model and used as BIM data for structural seismic analysis. Moreover, a program user could directly view, add, and modify Revit project parameter data at the Revit property bar interface. In order to realize rapid batch storage by the Revit redevelopment technology, file addresses of shared parameters, parameter group names, and parameter types were first set up to create a shared parameter file, which was then read to combine shared parameters with model elements and project parameters for specified families. Finally, project parameters were assigned values, and analysis data were stored in corresponding model elements. Seismic evaluation results of any component could be viewed at the property bar interface of Revit. The detailed algorithm of the aforesaid process is shown in Figure 9.

3.6. Summary of the Procedure of RTO Program. The procedure for using RTO is given according to individual steps 1–5 as follows:

TABLE 1: Strain-based seismic damage evaluation criteria of RC structural components and corresponding damage marking colors in the Revit model.

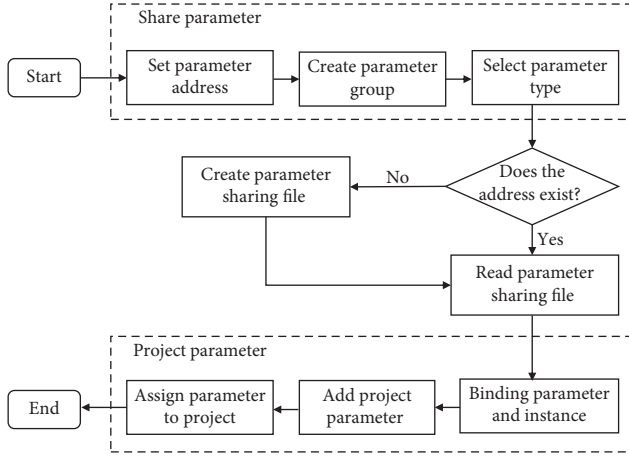| Damage level | Evaluation criterion | | Damage marking color |
	Concrete	Rebar	
Level 0	$|\varepsilon_2| \leq |\varepsilon_p|$	And $\varepsilon_1 < \varepsilon_y$	
Level 1	$|\varepsilon_2| \leq |\varepsilon_p|$	And $\varepsilon_y < \varepsilon_1 \leq 2\varepsilon_y$	
Level 2	$|\varepsilon_p| < |\varepsilon_2| \leq 1.5\,|\varepsilon_p|$	Or $2\varepsilon_y < \varepsilon_1 \leq 3.5\varepsilon_y$	
Level 3	$1.5|\varepsilon_{cp}| < |\varepsilon_2| \leq |\varepsilon_{cu}|$	Or $3.5\varepsilon_y < \varepsilon_1 \leq 12\varepsilon_y$	
Level 4	$|\varepsilon_2| > |\varepsilon_{cu}|$	Or $\varepsilon_1 > 12\varepsilon_y$	

FIGURE 9: Flowchart of project parameter storage of Revit.

(1) The building structure model was started up in Revit software

(2) The RTO program was started, the setups of analysis element, material mechanical properties, cross-section of components, structural constraint, vertical load, and the parameters of analysis and output were implemented, and then, the corresponding TCL command flow was automatically generated.

(3) The OpenSees program was called in the RTO program to read the TCL command flow generated in step 2, the finite element analysis was conducted, and the analysis data were outputted.

(4) According to the analysis requirements, the postprocessing was carried out for the output data of OpenSees, including plotting various curves, displaying tables, and outputting documents

(5) The seismic damage analysis was carried out according to the output data of OpenSees and seismic damage criterion, and then, the seismic damage level of each structural component of the considered structure was obtained. The obtained data on damage level were automatically stored in the corresponding structural component model of Revit, and the damage status was displayed in different feature colors.

4. Calculation Example

In this section, a calculation example was provided to demonstrate the operation process of the proposed method and the developed program, and some analysis results were discussed.

4.1. Example Model.
A five-story RC frame building was used as an example, and its Revit model is shown in Figure 10. The seismic fortification intensity was 8 (0.2 g), the site category was II, and the design group was the second group. The height of the first story model was 4.8 m, and the height of the other stories was 3.6 m. The frame plane layout is shown in Figure 11. The cross-sectional size of beams of each story was 250 mm × 500 mm. The longitudinal rebar area at the end cross-section of transverse beams was 1136.7 mm^2, and the rebar ratio was approximately 0.91%. The stirrup size of transverse beams was φ8@100/200. The longitudinal rebar area at the end cross-section of longitudinal beams was 1387.9 mm^2, and the rebar ratio was approximately 1.1%. The stirrup size of longitudinal beams was the same as that of transverse beams. The cross-sectional size of columns on each story was 450 mm × 450 mm. The longitudinal rebar area of columns was approximately 3768 mm^2, and the rebar ratio of the entire cross-section was approximately 1.86%. The configured stirrup size of columns was φ10@100/200. The strengths of longitudinal rebar, stirrup, and concrete were HRB335, HPB300, and C30, respectively. In the seismic design of the model building, the concepts of "strong columns and weak beams," "strong shear and weak bending," and "strong joints and weak components" were considered. It was assumed that joints were in an elastic state under strong earthquakes. When the example building was under strong earthquake, plastic hinges appeared at both ends of beams and columns, and this phenomenon could be simulated by the elastic-plastic fiber model.

4.2. Structural Seismic Analysis and Postprocessing.
For dynamic time history analysis, the EL Centro-180 ground motion record was chosen as the horizontal excitation of the example building, and the transverse direction (short side) of the building was chosen as the direction of seismic action. According to the levels of frequent earthquake (FE), moderate earthquake (ME), and rare earthquakes (RE), the peak acceleration amplitude of the selected seismic wave was changed to 70 gal, 196 gal, and 400 gal, respectively. Figures 12 and 13 show the program output dynamic time history curves of the roof displacement and the distribution curves of the maximum story drift under different seismic levels, respectively.
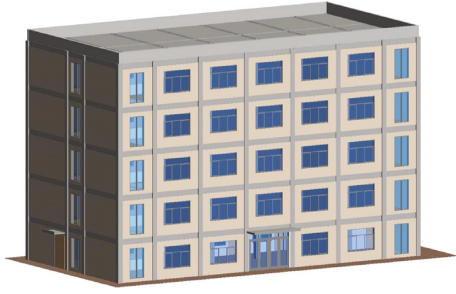
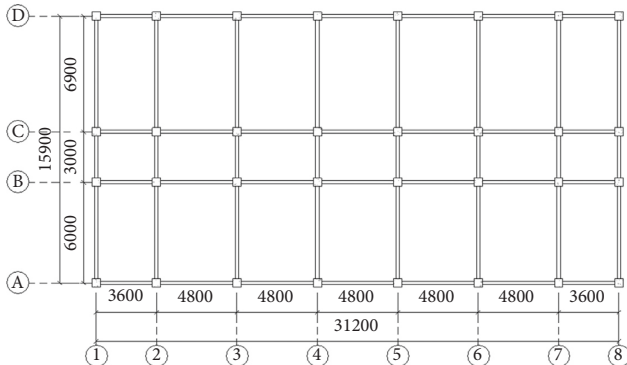FIGURE 10: Revit model of the example building.

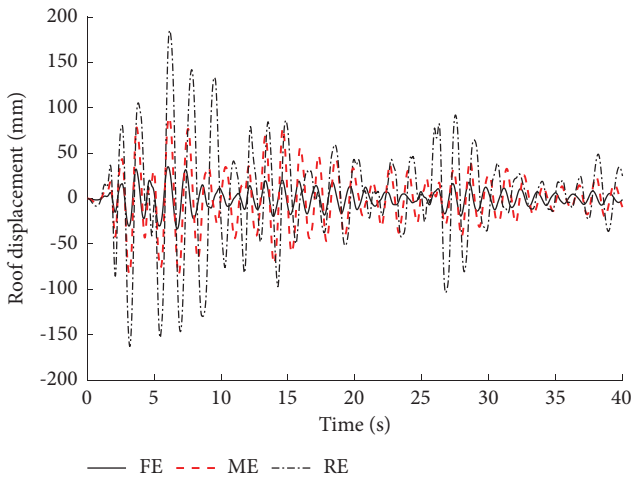FIGURE 11: Structural plan of the example building.

FIGURE 12: Dynamic time history curves of structural roof displacement for different earthquake levels.

As shown in Figure 13, under the action of rare earthquake level, the maximum story drift was approximately 0.0147, which is between the "basic operation" level (0.01) and the "life safety" level (0.02) and less than the limit of 1/50 given by the seismic code of China. Under the action of moderate earthquake level, the maximum story drift was approximately 0.0066, which is slightly less than the "basic operation" level (0.01), indicating that the considered building was in a stage of plastic reaction. Under the action of frequent earthquake level, the maximum story drift was
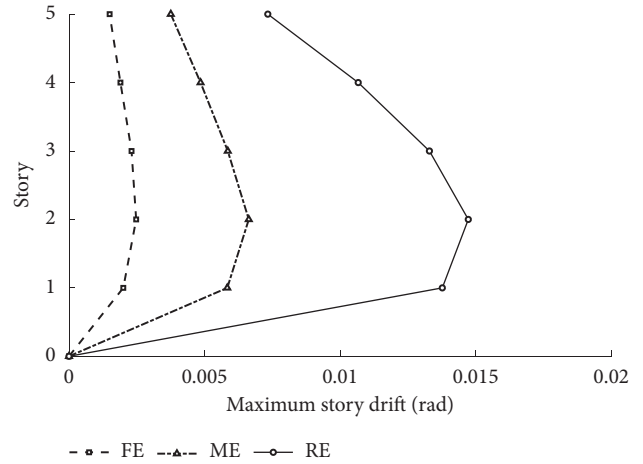

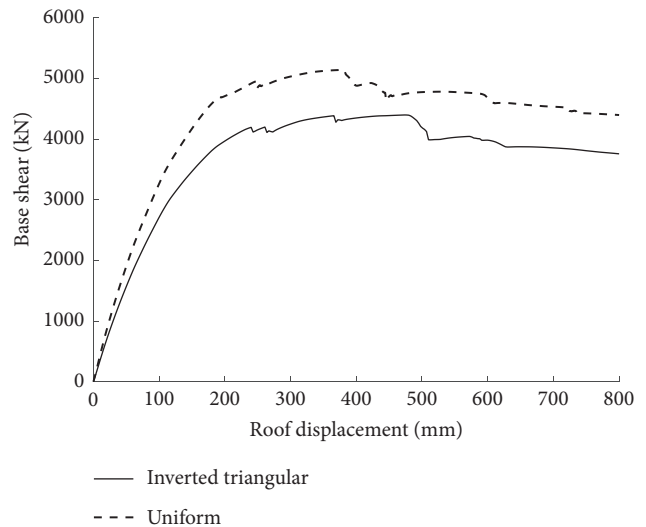FIGURE 13: Distribution curves of maximum story drifts for different earthquake levels.

FIGURE 14: Pushover capability curves for the two loading models.

approximately 0.0025, which is slightly greater than the limit of 1/550 given by the seismic code of China. The analysis model did not consider the impacts of enclosure and partition walls, whereas nonstructural components, such as filled walls, had great impacts on the elastic stiffness and period of the structure. When the structure experienced large plastic deformation, the walls lost their load-sustaining capability because of their brittleness. Therefore, the impact of the walls on structural responses was relatively small for the case of rare earthquake action. However, in the case of frequent earthquake action, the elastic stiffness of the structure was underestimated when walls were not set up in the model, resulting in a prolonged basic period and smaller structural responses.

The example building was subjected to a pushover analysis in the transverse horizontal direction. The capability curves of "roof displacement versus base shear" under the inverted triangle and uniform loading modes were calculated separately, and Figure 14 shows the

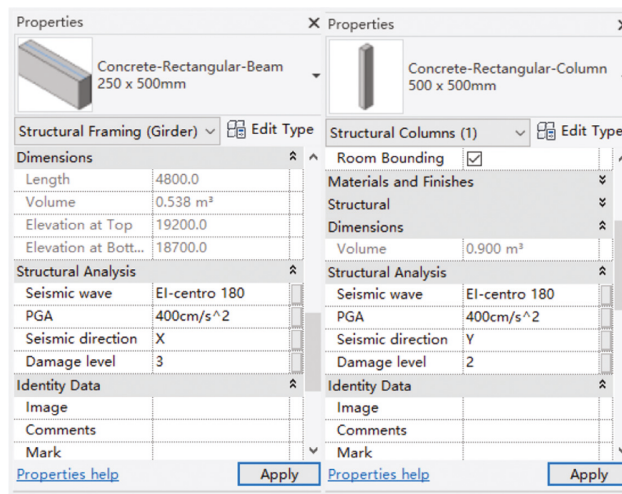Figure 15: Seismic damage information output.

Figure 16: Seismic damage information stored in Revit component model properties.

(a)

(b)
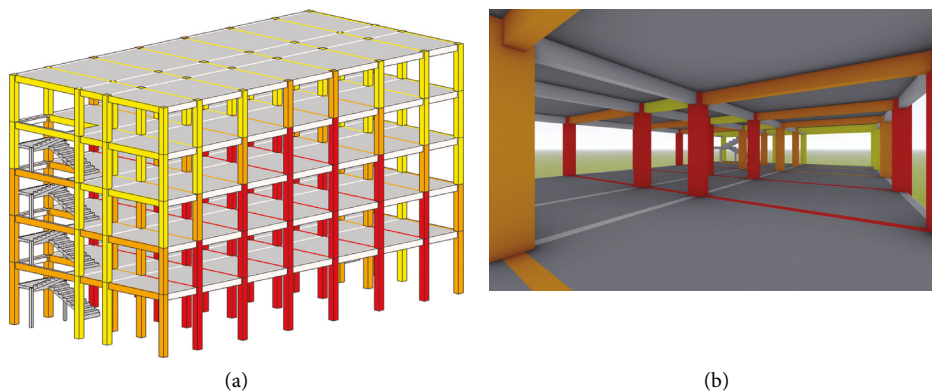
Figure 17: BIM visual display of seismic damage. (a) Three-dimensional view display. (b) Virtual roaming display.

capability curves for these two loading modes. A large difference could be seen in the capability curves obtained under the inverted triangle mode and the uniform mode. The reasons were as follows: according to horizontal static analysis, when the base shear was the same, the interstory shear generated by the inverted triangle loading mode was greater than that under the uniform loading mode, and the equivalent elastic stiffness of the structure under the inverted triangle loading mode was smaller than under the uniform loading mode; therefore, the roof displacement of former is greater than that of the latter in the elastic response stage. Moreover, due to this

large deformation, the structure under the inverted triangle loading mode entered the plastic response stage earlier, so the peak base shear under the inverted triangle loading mode was lower than that under the uniform loading mode.

4.3. Structural Seismic Damage Information Output. The strain data of longitudinal rebars and concrete in structural components were obtained by elastic-plastic analysis. The seismic damage level of each component was evaluated according to Table 1. The partial seismic performance information of the example structure is shown in Figure 15. Based on a secondary seismic damage analysis, damage information was automatically added to the attribute bar of each component in the Revit model (Figure 16).

In order to display structural seismic damage conditions in the Revit model, each component model was marked with the corresponding damage level color given in Table 1. Figure 17 shows the seismic damage condition of the example building under a rare earthquake level through the Revit 3D view and a virtual roaming. It is evident that the damage of columns was more serious than that of beams under the rare earthquake level. The proportions of beams with moderate damage (level 3), light-moderate damage (level 2), and slight damage (level 1) were 13.0%, 15.3%, and 17.6%, respectively. The corresponding values for columns were 38.7%, 27.5%, and 33.7%, respectively. The seismic damage of bottom-story columns was found to be the most serious.

5. Conclusions

A method of seismic analysis and damage evaluation was proposed, in which the data conversion between the BIM model and finite element model, parameter setting, calling of numerical analysis, data output and storage, and BIM visual display of seismic damage results were explored based on Revit platform, in order to realize the integration of seismic analysis of RC frame structures on BIM platform. The RTO program was developed through the Revit API interface using the C# language. The Revit to OpenSees conversion was carried out in Revit software to realize structural model data conversion, analysis parameter setup, analysis data postprocessing, and BIM storage of critical earthquake damage information. The main findings of this work are drawn as follows:

(1) The integration of a finite element program in the BIM platform was found to be feasible to analyze the seismic performance and evaluate the damage levels of RC frame structures. The proposed method provided a solution for seismic analysis and damage evaluation of RC frame structures to participate in BIM life cycle collaboration.

(2) The proposed method utilized the technical advantages of 3D view display and virtual roaming display in BIM to visually present the damage level and damage distribution of RC frame structures and components under earthquakes

(3) The proposed method allowed for the direct addition of structural component damage information under various earthquake levels to the BIM model, as well as the provision of expected seismic damage data for collaboration and structural operation and maintenance management of a building's life cycle in the BIM platform

Data Availability

The data used to support the findings of this study are available from the corresponding author upon request.

Conflicts of Interest

The authors declare that they have no conflicts of interest.

Acknowledgments

References

[1] C. Wan, P. H. Chen, and R. L. K. Tiong, "Assessment of IFCS for structural analysis domain," *Inform Technol Construction*, vol. 9, pp. 75–95, 2004.

[2] D. Yang, S. Yuan, and S. Ming, "Analysis on the application problems of BIM technology based on Revit in structural design," *Journal of Information Technology in Civil Engineering and Architecture*, vol. 6, pp. 13–18, 2014.

[3] I. J. Ramaji and A. M. Memari, "Information exchange standardization for BIM application to multi-story modular residential buildings," in *Proceedings of the AEI 2015: Conference on Birth and Life of the integrated Building*, pp. 13–24, Milwaukee, USA, 2015.

[4] H. Lai, X. Deng, and X. Liu, "IFC-based BIM data sharing and exchange," *Tumu Gongcheng Xue-bao/China Civil Engineering Journal*, vol. 51, no. 4, pp. 121–128, 2018.

[5] N. O. Nawari, "BIM data exchange standard for hydro-supported structures," *Journal of Architectural Engineering*, vol. 25, no. 3, Article ID 04019015, 2019.

[6] P. Mesároš, T. Mandičák, and A. Behúnová, "Use of BIM technology and impact on productivity in construction project management," *Wireless Networks*, vol. 28, no. 2, pp. 855–862, 2020.

[7] M.-A. Vigneault, C. Boton, H.-Y. Chong, and B. Cooper-Cooke, "An innovative framework of 5D BIM solutions for construction cost management: a systematic review," *Archives of Computational Methods in Engineering*, vol. 27, no. 4, pp. 1013–1030, 2020.

[8] A. M. M. Hasan, A. A. Torky, and Y. F. Rashed, "Geometrically accurate structural analysis models in BIM-centered software," *Automation in Construction*, vol. 104, pp. 299–321, 2019.

[9] I. J. Ramaji, J. I. Messner, and E. Mostavi, "IFC-based BIM-to-BEM model transformation," *Journal of Computing in Civil Engineering*, vol. 34, no. 3, Article ID 04020005, 2020.

[10] A. Khalili, "An XML-based approach for geo-semantic data exchange from BIM to VR applications," *Automation in Construction*, vol. 121, Article ID 103425, 2021.

[11] X. Zeng, X. Z. Lu, and Z. Xu, "Modeling technology for building aseismic elasto-plastic analysis based on BIM data," *Computer Aided Engineering*, vol. 23, no. 4, pp. 5–11, 2014, in Chinese.

[12] L. Barazzetti, F. Banfi, R. Brumana, G. Gusmeroli, M. Previtali, and G. Schiantarelli, "Cloud-to-BIM-to-FEM: structural simulation with accurate historic BIM from laser scans," *Simulation Modelling Practice and Theory*, vol. 57, pp. 71–87, 2015.

[13] L. C. Dong, P. H. Huang, and T. Ozbakkaloglu, "The research of design method of building structure based on BIM," *AER-Advances in Engineering Research*, vol. 72, pp. 537–540, 2016.

[14] S. Tafraout, N. Bourahla, Y. Bourahla, and A. Mebarki, "Automatic structural design of RC wall-slab buildings using a genetic algorithm with application in BIM environment," *Automation in Construction*, vol. 106, Article ID 102901, 2019.

[15] Z. Xu, Z. Zhang, X. Lu, X. Zeng, and H. Guan, "Post-earthquake fire simulation considering overall seismic damage of sprinkler systems based on BIM and FEMA P-58," *Automation in Construction*, vol. 90, pp. 9–22, 2018.

[16] J. Shi, J. Dao, L. Jiang, and Z Pan, "Research on IFC- and FDS-based information sharing for building fire safety analysis," *Advances in Civil Engineering*, vol. 2019, no. 2, 18 pages, Article ID 3604369, 2019.

[17] J. C. Lee, "IFC structural information model for practical use of OpenSees," *Journal Of The Architectural Instutute Of Korea Structure and Construction*, vol. 28, no. 12, pp. 53–60, 2012.

[18] M. Alirezaei, M. Noori, O. Tatari, K. R. Mackie, and A. Elgamal, "BIM-based damage estimation of buildings under earthquake loading condition," *Procedia Engineering*, vol. 145, pp. 1051–1058, 2016.

[19] E. B. Anil, B. Akinci, O. Kurc, and J. H. Garrett, "Building-information-modeling–based earthquake damage assessment for reinforced concrete walls," *Journal of Computing in Civil Engineering*, vol. 30, no. 4, Article ID 04015076, 2016.

[20] D. Zou, K. Chen, X. Kong, and X. Yu, "An approach integrating BIM, octree and FEM-SBFEM for highly efficient modeling and seismic damage analysis of building structures," *Engineering Analysis with Boundary Elements*, vol. 104, pp. 332–346, 2019.

[21] D. Perrone and A. Filiatrault, "Automated seismic design of non-structural elements with building information modelling," *Automation in Construction*, vol. 84, pp. 166–175, 2017.

[22] U. Vitiello, V. Ciotta, A. Salzano, D. Asprone, G. Manfredi, and E Cosenza, "BIM-based approach for the cost-optimization of seismic retrofit strategies on existing buildings," *Automation in Construction*, vol. 98, pp. 90–101, 2019.

[23] Z. Xu, H. Zhang, X. Lu, Y. Xu, Z. Zhang, and Y. Li, "A prediction method of building seismic loss based on BIM and FEMA P-58," *Automation in Construction*, vol. 102, pp. 245–257, 2019.

[24] Z. Xu, X. Lu, X. Zeng, Y. Xu, and Y. Li, "Seismic loss assessment for buildings with various-LOD BIM data," *Advanced Engineering Informatics*, vol. 39, pp. 112–126, 2019.

[25] Z. Xu, F. R. Zhang, W. Jin, Y. Wu, M. Qi, and Y. Yang, "A 5D simulation method on post-earthquake repair process of buildings based on BIM," *Earthquake Engineering and Engineering Vibration*, vol. 19, no. 3, pp. 541–560, 2020.

[26] N. Caterino, I. Nuzzo, A. Ianniello, G. Varchetta, and E. Cosenza, "A BIM-based decision-making framework for optimal seismic retrofit of existing buildings," *Engineering Structures*, vol. 242, no. 3, Article ID 112544, 2021.

[27] R. Zeibak-Shini, R. Sacks, L. Ma, and S. Filin, "Towards generation of as-damaged BIM models using laser-scanning and as-built BIM: first estimate of as-damaged locations of reinforced concrete frame members in masonry infill structures," *Advanced Engineering Informatics*, vol. 30, pp. 312–326, 2016.

[28] C. Musella, M. Serra, C. Menna, and D. Asprone, "Building information modeling and artificial intelligence: advanced technologies for the digitalisation of seismic damage in existing buildings," *Structural Concrete*, vol. 22, no. 5, pp. 2761–2774, 2021.

[29] M. Chen, "Composition and advantages of three tier architecture," *Information and Communications*, vol. 33, no. 1, pp. 147-148, 2020, in Chinese.

[30] National Standard of the People's Republic of China, *GB/T 38591-2020, Standard for Seismic Resilience Assessment of buildings*, China Standard Press, Beijing, China, 2020, in Chinese.